Cell damage extent due to irradiation with nanosecond laser pulses under cell culturing medium and dry environment

Francisco G. Pérez-Gutiérrez[1], Gabriel Guillen[2], Rodger Evans[3]
Santiago Camacho-López[3], Guillermo Aguilar[1]
1. Department of Mechanical Engineering, University of California, Riverside; 900 University Ave, Riverside, CA, USA 92521.
2. Instituto de Biotecnología, Universidad Nacional Autónoma de México; Av. Universidad #2001, Col.Chamilpa C.P. 62210 Cuernavaca, Morelos, México.
3. Departamento de Óptica, Centro de Investigación Científica y de Educación Superior de Ensenada; Km. 107 Carretera Tijuana - Ensenada C.P. 22860, Ensenada, B.C., México.

ABSTRACT

Cell mono-layers were irradiated with nanosecond laser pulses under two distinct scenarios: (a) with culturing medium positioning the beam waist at different stand-off distances γ and (b) without cell culturing medium, positioning the beam waist directly on top of the cell mono-layer. Damaged cells were marked with Trypan Blue, a vital cell marker. Three different zones of damage were identified: (1) a zone of complete cell clearance, surrounded by (2) a ring of dead cells marked with Trypan Blue and (3) the rest of the cell culture where the cells remain alive and viable. Different hydrodynamic mechanisms damage cells as it was shown by high speed video for γ=0 and comparison with time resolved imaging. The cell damage mechanism has its origin on the optical breakdown plasma formation. For the case with culturing medium, a combination of plasma formation and shear stresses are responsible for cell damage; wheras for the case without cell culturing medium, the plasma formation is the only mechanism of interaction between laser pulses and cells. The rapidly expanding plasma generates shock waves whose pressure is most likely responsible for the cell detachment observed.

Keywords: nanosecond laser pulses, cell damage extent, optical breakdown, shear stresses, water jet, bubble dynamics.

1. INTRODUCTION

Interactions of short laser pulses with biological materials and tissues have been thoroughly studied during the last two decades because of its characteristics of producing material ablation with minimal thermal damage effects to the surrounding material. Such unique qualities make short laser pulses very appealing for medical applications [1-4]. The most common materials used as experimental models of biological tissue are water, polyacrylamide and agar gels because its thermal properties are very similar to those of real tissue and its optical and mechanical properties can easily be adjusted by means of changes in water content and dyes [2, 5-8].

When a nanosecond-long laser pulse is tightly focused in the bulk of a liquid medium or a gel and it is intense enough to produce optical breakdown, the rapidly expanding plasma leads to a bubble formation phenomenon preceded by a shock wave launch [2-4, 9-11]. When the plasma is formed in liquid environment, the bubble size presents and oscillatory behavior where several growth stages and collapses can be observed before the bubble disappears. In the case of gels, the oscillatory behavior can be observed when the pressure inside the bubble does not overcome the gel's elastic modulus, otherwise, a bubble whose size does not change with time remains in the gel [2, 5, 6]. The first stage of bubble formation and shock wave propagation occurs in nanosecond time scale, therefore sophisticated high speed video or time resolved (shadowgraphy or laser photography) imaging systems are required to study them [3, 5, 9].

Optical Interactions with Tissue and Cells XX, edited by Steven L. Jacques, E. Duco Jansen, William P. Roach,
Proc. of SPIE Vol. 7175, 717514 · © 2009 SPIE · CCC code: 1605-7422/09/$18 · doi: 10.1117/12.816562

When a bubble is generated near a solid boundary, the transient oscillatory flow around the bubble interacts with the solid surface. The collapse near a solid boundary is followed by the formation of a liquid jet in the direction of the boundary and a ring vortex formation after the first collapse. Cavitation erosion by single laser-produced bubbles has been studied in the past [10]. In this work the different stages of the bubble dynamics near a solid boundary are found to play a role in the surface erosion at different stand-off distances γ, defined as $\gamma=h/R_{max}$, where h is the distance from the surface to the bubble center and R_{max} is the maximum radius of the bubble.

The interaction of the flow surrounding the bubble and a solid boundary produces shear stresses that may also play a role on the mechanisms of damage [12-14]. In this work, the damage extent of a monolayer cell culture is compared when it is irradiated with focused laser pulses for samples with and without culture media on top of the cells; the cell damage mechanism has its origin on the optical breakdown plasma formation for the first case, while a combination of plasma formation and shear stresses are responsible for cell damage in the second case. Special attention is given to the case where $\gamma=0$ for different laser pulse energies.

2. MATERIALS AND METHODS

2.1 Laser system and Experimental Setup

The experimental set up used for this work is shown in Fig 1. It consists of a Q-switched, 532 nm, Nd:YAG, emitting 6 ns long laser pulses. The laser beam was tightly focused using an f_1=8 mm, NA=0.5, aspheric lens (L1). The beam waist was positioned at a desired position by means of an Equivalent Target Plane (ETP) system which consisted on a CCD camera to capture the image of the focused beam on the target; this was done by using an image relay system constituted by the L1 lens and the f_2=250 mm lens (L2); the light that reflects backwards from the sample surface was collected by the two lenses projecting a magnified ($M=f_2/f_1$) image of the beam waist onto the CCD. This image relay system provided two very useful features to our set up: (1) it required normal incidence to work so that the sample surface was always perpendicular to the incident beam, and therefore, in the event of a transversal scan of the sample the beam waist of the focusing light stayed always at a constant distance from the surface; (2) it allowed fine positioning of the beam waist right on the surface of the sample, and hence at a known depth within the layer, with a resolution of the order of the Rayleigh range (~20 μm) of the focusing beam. The sample was mounted on a micrometer-driven translation stage that allowed precise positioning (~ 5 μm resolution) of the sample with respect to the L1 lens. Laser energy per pulse was recorded by means of an energy monitor (EM) previously calibrated against a second energy meter.

2.2 Lateral visualization of bubble growth:

Lateral visualization of the bubble formation phenomena is performed with a Phantom high speed camera (HS). HS camera settings were 66,666 fps with 2 μs exposure time and 128 x 128 pixels for spatial resolution. Such parameters were chosen so both, time scale and spatial resolution, are enough to visualize bubble formation. Although the frame rate is poor to visualize shock wave formation and bubble growth for energies below 400 μJ, it allowed bubble growth identification for higher energies. From there, the maximum bubble sizes as a function of energy were obtained.

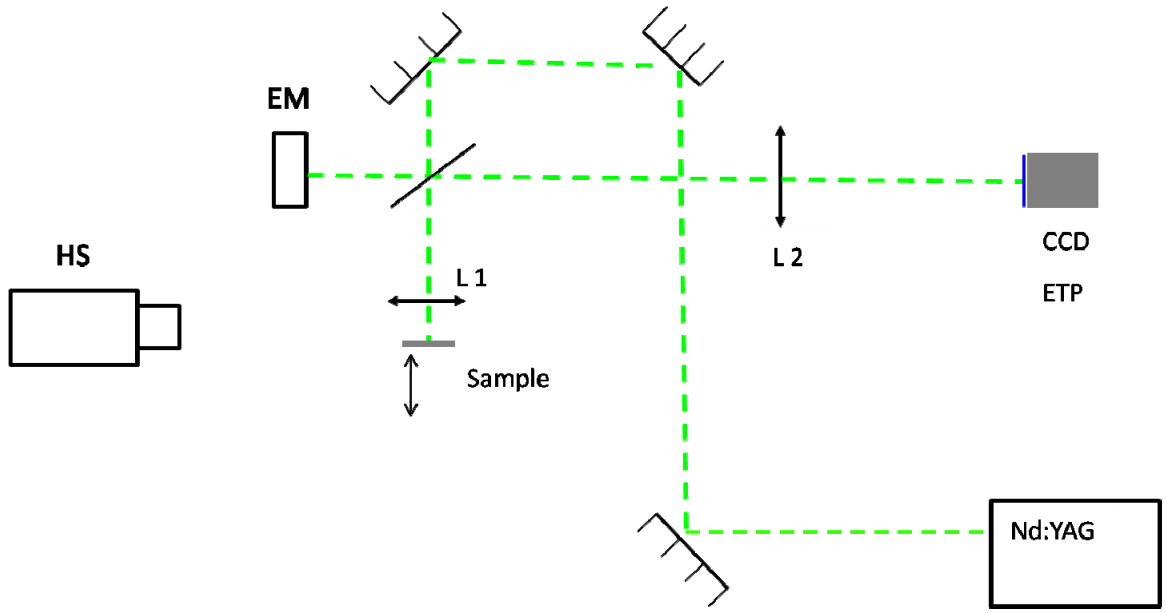

Fig. 1. Experimental setup used for irradiation of cell mono-layers. Laser system is a Q-switched, λ=532 nm, Nd:YAG, 6 ns pulse duration. L1 is a f=8 mm NA=0.5 aspheric lens; L2 is a f=250 mm convex lens. High speed video settings are 66,666 fps, exposure time 2 μs.

2.3 Laser irradiation

Cell monolayers were irradiated with nanosecond laser pulses under two different scenarios: (1) culture medium was totally removed from cells so focused laser pulses directly interacted with cell monolayers, shown in Fig 2A; (2) laser pulses were focused within the culture medium varying the stand-off distance γ, shown in Fig 2B. For the first scenario the laser pulse energy was varied from 100 μJ up to 1 mJ and for the second was fixed at 1 mJ± 10%.

For precise positioning of the beam waist, the refractive index of the culture medium was experimentally determined to be 1.74. Using Snell's law, the relative distance between the beam waist and the sample surface was calculated so that the stand-off distance (γ) is correctly determined taking into account the beam deflection when it interacts with the cell culture medium. In all cases, γ was calculated by dividing the h distance, at which the beam waist was positioned, and R_{max} corresponding to the incident pulse energy recorded in each experiment.

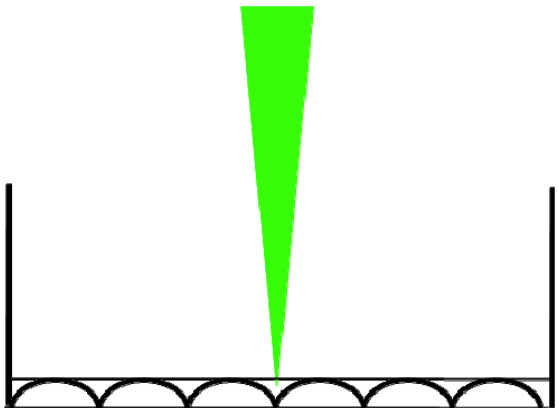

Fig. 2A. Geometry of cell irradiation without cell culturing medium. Horizontal line on top cells indicates the cell mono-layer surface.

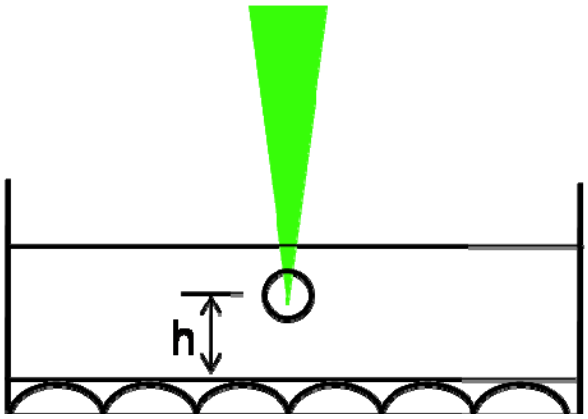

Fig. 2B. Geometry of cell irradiation with cell culturing medium. Horizontal line on top cells indicates the cell mono-layer surface.

2.4 Cell culturing and cell viability determination

SF9 cells, an adherent cell line, were cultured in suspension with Sf-900 II SFM media at 28 ^{o}C. Later, 1.5 x 10^{6} cell/ml were seeded as monolayers on 6-well tissue treated clusters. Cells were incubated for at least 12 hrs before the experiment to ensure uniform cell attachment to the surface.

Right after laser irradiation, a 0.08% solution of Trypan Blue, a vital dye, was added to the samples. The reactivity of Trypan Blue is based on the fact that the chromophore is negatively charged and does not interact with the cell unless the membrane is damaged. Therefore, all cells which exclude the dye are viable. Control samples were kept without laser irradiation during the experiment. Cells with Trypan Blue were observed using an inverted microscope with 10X and 5X objectives.

3. RESULTS AND DISCUSSION

Figure 3A and 3B show cell mono-layers irradiated with focused nanosecond laser pulses with and without culture media on top of the cells, respectively. In both figures, three main regions can be identified: (1) a zone of complete cell clearance, surrounded by (2) a ring of dead cells marked with Trypan Blue and (3) the rest of the cell culture where the cells remain alive and viable. In general, the ring of dead cells was thinner for cells irradiated in a dry environment than that of cells irradiated in culturing medium. Pictures of cells irradiated without cell culture medium were taken with 10X objective; the region affected on cells irradiated in cell culture medium was larger than that of the cells irradiated without culturing medium, therefore pictures were obtained using a 5X objective. Pictures of cell monolayers irradiated without cell culturing medium show optical damage of the cell culturing plastic well; this is because the beam waist was positioned on top of the cells, the Rayleigh range of the focused beam is 20 μm, which is the thickness of the cell mono-layer (approximately 20 μm); therefore it is not surprising that the highest intensity of the laser beam reaches both the cell monolayer and the cell culturing plastic well. Previous works report the shock wave that a rapidly expanding plasma generated by focused nanosecond laser produces [2-5, 11], which is the most likely mechanism responsible for the cell detachment observed.

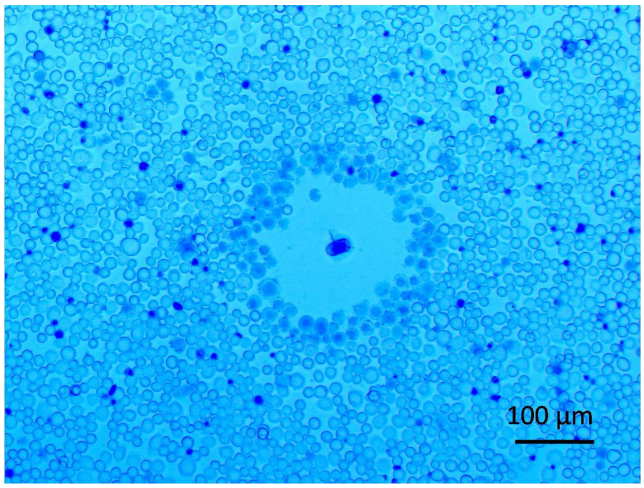

Fig. 3A. Cell monolayer without culture media irradiated with nanosecond laser pulses focused directly on the cell layer. Image obtained with a 10X microscope objective.

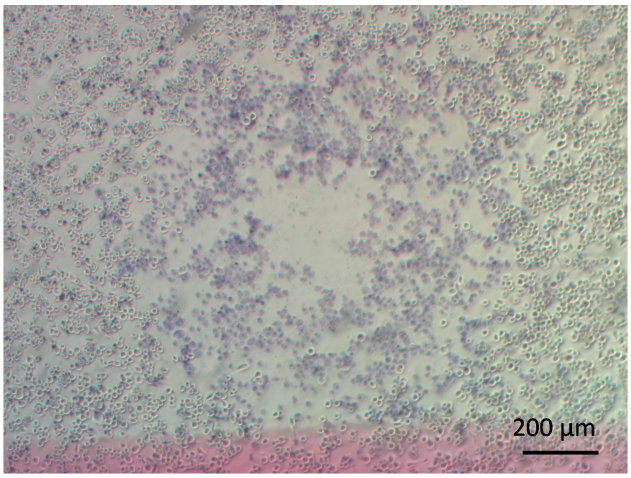

Fig. 3B. Cell monolayer with culture medium on top of cells irradiated with nanosecond laser pulses. The beam waist was positioned at a stand-off distance γ=0. Image obtained with a 5X objective.

Figure 4 shows a laser-induced bubble at its maximum photographed size. Laser beam was focused at the surface of the sample. Bubbles induced by laser pulses with energy smaller than 400 µJ could not be recorded as its life time is probably shorter than the time resolution available with the HS camera.

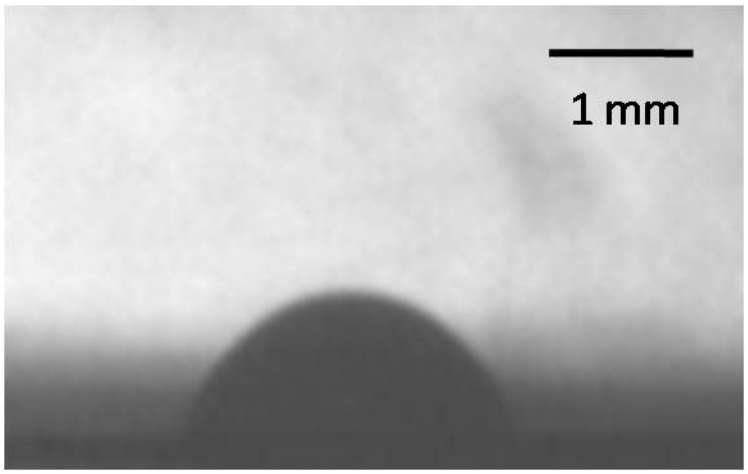

Fig. 4. Laser induced bubble in cell culture at γ=0. Bubble photographed at its maximum captured size. The laser pulse energy was 823 µJ.

Figure 5 shows a comparison of the cell damage extent when the cell mono-layers with and without cell culture medium were irradiated, and the maximum bubble diameter as a function of the laser pulse energy when γ=0. Cell damage extent with and without cell culture medium have the same trend below 400 µJ, and both continue increasing with laser pulse energy. The cell damage extent without cell culture medium increases with an asymptotic trend for higher laser pulse energies, whereas cell damage extent with culturing medium seems to continue monotonically increasing with laser pulse energy, presumably due to the shear stresses generated by the interaction of the bubble wall with the cell mono-layer and further transient flow field surrounding the bubble. Interestingly, the bubble maximum diameter coincides with

cell damage extent for samples with cell culturing medium, see Figure 5. Unfortunately, the time resolution did not allow imaging of bubbles generated by laser pulses with energy lower than 400 μJ, because its life time is shorter than what the video settings allowed to record.

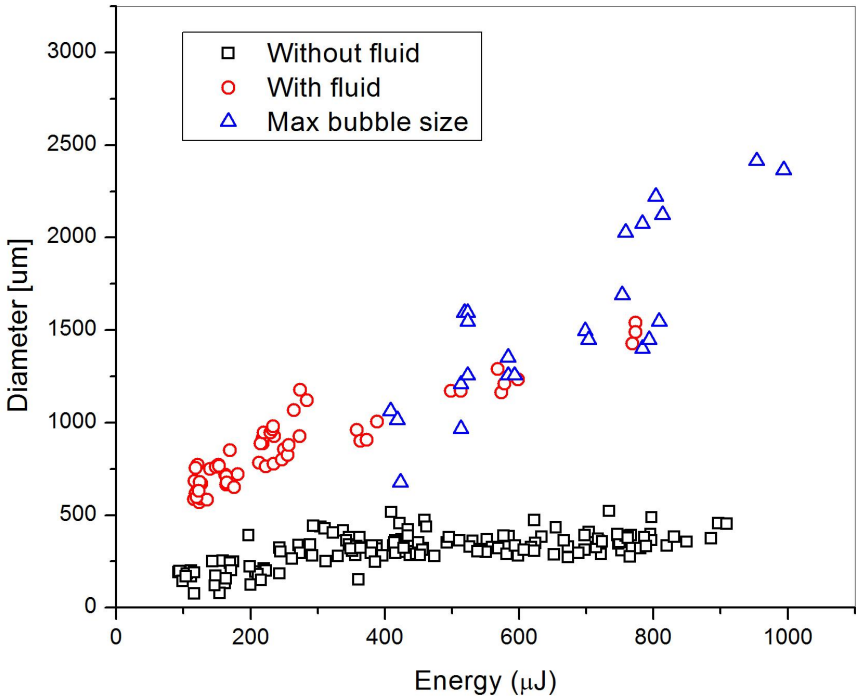

Fig. 5. Comparison of cell culture damage extent for samples irradiated with and without cell culturing medium and maximum bubble size, all when γ=0.

Figure 6 presents the cell damage extent zone diameter that encloses both the area of total cell clearance and the ring of dead cells that were not detached from the plastic well marked with Trypan Blue, normalized with respect to the maximum size of damage extent. Cell damage extent increases with γ for $0<\gamma<0.6$, until cell damage extent reaches its maximum and then decreases until a local minimum for $0.6<\gamma<1.9$. For γ=0, cell damage extent is 58% of the maximum damage extent size, and for γ=1.9 it is 37%. These results are consistent with a recent study [12] where a similar experiment was carried out with adherent HeLa cells, where a similar behavior for $0<\gamma<2$ was found, being γ=0.65 the stand-off distance at which damage extent is maximum in the cell culture. However in our case, damage was found for $\gamma>2$ without a well defined trend, being γ=5 the stand-off distance for which damage to the cell ceulture stops. Other authors studied cavitation erosion by single laser-produced bubbles in a fluid over metallic surfaces [10]; they also found erosion of the surface for $0<\gamma<2$ when several pulse are delivered.

The discrepancy between the results in this work and published data might be due to differences in the multiple optical parameters involved during the irradiation process, as well as the culturing medium and cell line used. It is likely that the SF9 cell line does not adhere to the plastic well as strongly as HeLa cells do. Another study presents a thorough analysis of time resolved images of bubble dynamics near a solid boundary for different γ values [11], which will be referred throughout this discussion.

For $0<\gamma<0.75$, there is direct interaction of the bubble wall with the surface. For γ values greater but very close to zero, the damage mechanism is a combination of the expanding plasma acting directly on the cell mono-layer and bubble wall

interaction with the solid surface; this statement is supported by Figure 5 where there is overlapping of the maximum bubble diameter with cell damage extent when γ=0.

For greater values of γ and up to 1 (pictures in the referred work are shown at γ=0.75), where there is no interaction of plasma with cells, there are two possible damage mechanisms: (1) the shear stresses due to the interaction of the bubble wall and the cells and (2) the shear stresses due to the flow field induced by the bubble wall in the fluid surrounding the bubble near the surface [14].

For γ>1 the bubble wall does not touch the solid surface during the first expansion-compression period, but instead, there is formation of a liquid jet in the direction of the boundary and a ring vortex formation after the first collapse, the bubble distorts from its original shape and is pulled down in the direction of the water jet, producing the so called water hammer, which has been proven to be a mechanism producing erosion on solid surfaces [10]; this is the mechanism damaging cells for this γ range.

It is shown that for γ=2.3, the water jet that forms after the first collapse barely touches the surface; therefore, for γ>2 the shear stresses induced by the flow field due to bubble formation must produce greater contribution to the cell damage than the water jet under these circumstances, as the experimental data presented here suggest. If SF9 cell adhesion to the surface is weak, it is likely that some damage extent may be produced by these shear stresses.

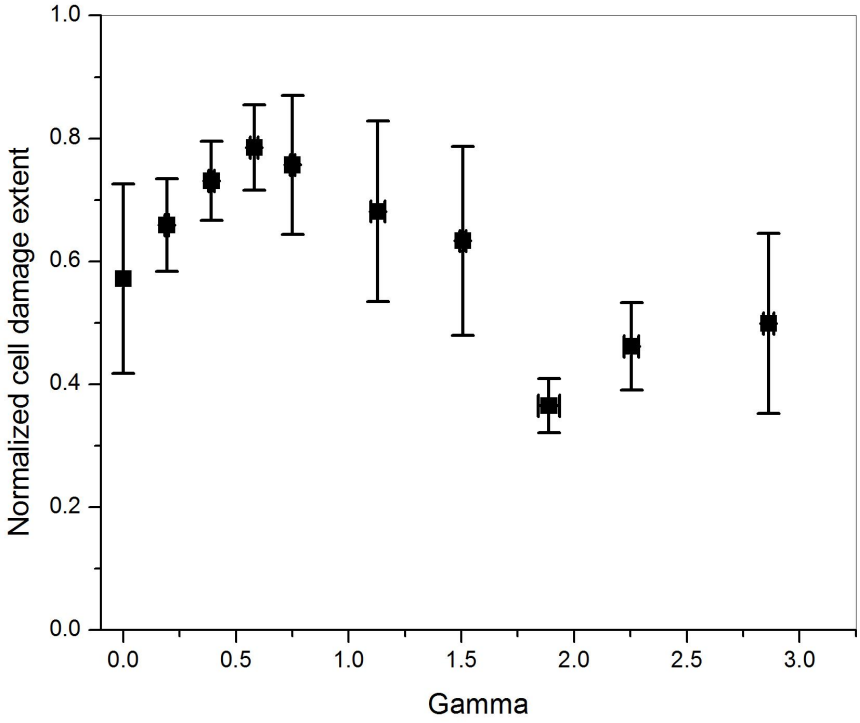

Fig. 6. Normalized cell damage extent diameter as a function of the stand-off distance γ, when cell mono-layers are irradiated with culturing medium on top. Laser energy was 1 mJ ± 10%, which leaded to bubble radius of 0.59 mm ± 10%.

4. CONCLUSIONS

Cell mono-layers were irradiated with nanosecond laser pulses under two distinct scenarios: (1) with culturing medium positioning the beam waist at different stand-off distances γ and (2) without cell culturing medium, positioning the beam

waist directly on top of the cell mono-layer. Three different zones of damage were identified: (1) a zone of complete cell clearance, surrounded by (2) a ring of dead cells marked with Trypan Blue and (3) the rest of the cell culture where the cells remain live and viable. For the first case, cell damage extent encloses the first two zones and varies with γ to a local maximum at γ=0.6 and a local minimum at γ=1.9; for γ>2 there is some damage extent most likely due to shear stresses induced by bubble dynamics; discrepancies with published data may be attributed to the fact that SF9 cells do not adhere to plastic wells as strong as HeLa cells do. Different hydrodynamic mechanisms damage cells as it was shown by high speed video for γ=0 and comparison with time resolved imaging previously reported. For the case without culturing medium, the plasma formation is the only mechanism of interaction between laser pulses and cells. The rapidly expanding plasma generates shock waves whose abrupt (nanosecond risetime) highpressure is most likely responsible for the cell detachment observed.

5. AKNOWLEGMENTS

The authors thank Dr. Rosaura Aparicio Fabre for her assistance with cell culturing and Mr. Edgar Arturo Chávez Urbiola for his help during the experiments. UCMEXUS-CONACyT scholarship for graduate studies for FGPG and DGAPA-UNAM support for GG are greatly appreciated. Also, CONACyT-Ciencia Básica grant 57309 and UCR Academic Senate, Committee on Research Fellowships 2008-2009 provided financial support for this work.

6. REFERENCES

[1] Vogel, A., and Venugopalan, V., "Mechanisms of Pulsed Laser Ablation of Biological Tissues," Chem. Rev., 103, 577-644 (2003).
[2] Brujan, E. A., Vogel, A., "Stress wave emission and cavitation bubble dynamics by nanosecond optical breakdown in a tissue phantom," J. Fluid Mech., 558, 281-308 (2006).
[3] Vogel, A., Busch, S., "Shock wave emission and cavitation bubble generation by picosecond and nanosecond optical breakdown in water," J. Acoust. Soc. Am., 100(1), 148-165 (1996).
[4] Vogel, A., Lauterborn, W., "Acoustic transient generation by laser-produced cavitation bubbles near solid boundaries," J. Acoust. Soc. Am., 82(2), 719-731 (1998).
[5] Evans, R., Camacho-Lopez, S., Perez-Gutierrez, F. G., Aguilar, G., "Pump-probe imaging of nanosecond laser-induced bubbles in agar gel," Optics Express, 16(10), 7481-7492 (2008).
[6] Pérez-Gutiérrez, F. G., Evans, R., Camacho-Lopez, S., Aguilar, G., "Short and ultrashort laser pulse induced bubbles on transparent and scattering tissue models," Proc. of SPIE 6435, 1-8 (2007).
[7] Oraevsky, A., Jacques, S. L., "Mechanisms of laser ablation for aqueous media irradiated under confined-stress conditions," J. Appl. Phys, 78(2), 1281-1290 (1995).
[8] Oraevsky, A. A., Jacques, S. L., Esenaliev, R. O., Tittel, F. K., "Pulsed Laser Ablation of Soft Tissues, Gels and Aqueous Solutions at Temperatures Below 100 C," Lasers in Suergery and Medicine, 8, 231-240 (1996).
[9] Ohl, C. D., Kurz, T., Geisler, R., Lindau, O., Lauterborn, W., "Bubble dynamics, shock wave and sonoluminescence," Phil. Trans. R. Soc. Lond. A., 357, 269-294 (1999).
[10] Philipp, A., Lauterborn, W., "Cavitation erosion by single laser-produced bubbles," J. Fluid Mech., 361, 75-116 (1998).
[11] Vogel, A., Lauterborn, W., Timm, R., "Optical and acoustical investigations of the dynamics of laser-produced cavitation bubbles near a solid boundary," J. Fluid Mech., 206, 299-338 (1989).
[12] Dijkink, R., Gac, S. L., Nijhuis, E., Berg, A. v. d., Vermes, I., Poot, A., Ohl, C. D., "Controlled Cavitation-cell interaction: trans-membrane transport and viability studies," Phys. Med. Biol., 53, 375-390 (2008).
[13] Rau, K. R., III, A. G., Vogel, A., Venugopalan, V., "Investigation of laser-induced cell lysis using time-resolved imaging," Applied Physics Letters, 84(15), 2940-2942 (2004).
[14] Rau, K. R., Quinto-Su, P. A., Hellman, A., Venugopalan, V., "Pulsed Laser Microbeam-Induced Cell Lysis: Time-Resolved Imaging and Analysis of Hydrodynamical Effects," Biophysical Journal, 91, 371-329 (2006).